Biomedical Signal Processing and Control 89 (2024) 105803

Contents lists available at ScienceDirect

Biomedical Signal Processing and Control

journal homepage: www.elsevier.com/locate/bspc

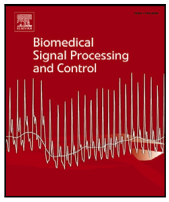

Variable structure based control strategy for treatment of HCV infection

Ali Hamza [a], Muhammad Uneeb [b], Iftikhar Ahmad [b], Komal Saleem [a], Zunaib Ali [a,*]

[a] London Center of Energy Engineering (LCEE), School of Engineering, London South Bank University (LSBU), United Kingdom
[b] Department of Electrical Engineering, School of Electrical Engineering and Computer Science, National University of Sciences and Technology (NUST), Islamabad, Pakistan

ARTICLE INFO

Keywords:
Hepatitis C Virus
Integral Sliding Mode Controller (ISMC)
Double Integral Sliding Mode Controller (DISMC)
Integral Terminal Sliding Mode Controller (ITSMC)
Fractional Order Terminal Sliding Mode Controller (FOTSMC)

ABSTRACT

Hepatitis C is such a harmful disease which can lead to serious health problems and it is caused by the Hepatitis C Virus (HCV) which causes liver inflammation and sometimes liver cancer. In this work, the control treatment strategy for HCV infection has been proposed. The advanced nonlinear dynamical mathematical model of HCV that has two control inputs and three state variables such as virions, infected hepatocytes and uninfected hepatocytes are considered for controller design in this research work. Moreover, four nonlinear controllers such as the Fractional Order Terminal Sliding Mode Controller (FOTSMC), Integral Terminal Sliding Mode Controller (ITSMC), Double Integral Sliding Mode Controller (DISMC) and Integral Sliding Mode Controller (ISMC) have been proposed in this work for HCV infection control inside the human body. In order to control the amount of uninfected hepatocytes to its required maximum safe limit, controllers are designed for antiviral therapy in which the amount of virions and infected hepatocytes are tracked to zero. One control input is ribavirin which blocks virions production and the other is pegylated interferon (peg-IFN-α) that acts as reducing infected hepatocytes. By doing so, uninfected hepatocytes increase and achieve the required maximum safe limit. To prove the stability of the whole system, Lyapunov stability analysis is used in this work. Simulation results and comparative analysis are carried out by using MATLAB/Simulink. It can be depicted from the given results that the virions and infected hepatocytes are reduced to their required levels completely using FOTSMC and the Sustained Virologic Response (SVR) rate is also enhanced in it. It reduces the treatment period as compared to previous strategies introduced in the literature and also system behaves very nicely even in the presence of un-modeled disturbances.

1. Introduction

Hepatitis C Virus (HCV) is the most commonly known liver disease which was first identified in 1989. Serological tests are used to discover Hepatitis A Virus (HAV) and Hepatitis B Virus (HBV) during the 1970s and 1980s. Further research has discovered some Non-A, Non-B Hepatitis (NANBH) that are not associated with HAV or HBV. This particular clone came to be named as HCV [1]. World Health Organization published a report in 2017 in which it was illustrated that almost 71 million people had been experiencing HCV infection globally. Nearly 14 million people were diagnosed with HCV infection but only 1.1 million patients had gotten proper treatment [2]. HCV is a positive-strand Ribonucleic Acid (RNA) virus because it belongs to the Hepacivirus genus and Flaviviridae family.

Researchers started their efforts to analyze the kinetic modeling of the HCV virus after its discovery in the late 20th century. Neumann proposed very first mathematical model in [3] which was adopted from HIV infections [4] and HBV [5]. Interferon-based treatment was carried out through this model. The production rate of virions was blocked by it. It affected healthy cells a little bit. By the inclusion of the effect of ribavirin in [3], the impact of peg-IFN-α was improved of peg-IFN-α in [6]. This model worked in two phases; during the first phase, it was depicted that peg-IFN-α was used that had great importance and the virus declined, while during the second phase in the presence of low peg-IFN-α efficacy, a significant contribution was made by ribavirin. A new model was proposed in [7] that had a tri-phasic declining pattern of viral load. Under DAAS [8–12], some novice dynamical models for HCV have been proposed in recent times. To develop further novice models for stimulating therapeutic cells, various studies have been conducted by considering the role of the immune system and these cells reduce viral load [13–16].

A wide range of applications in ecological and biological problems have been found through control theory [17]. A nonlinear controller

* Corresponding author.
E-mail addresses: hamzaa10@lsbu.ac.uk (A. Hamza), muneeb.msee17seecs@seecs.edu.pk (M. Uneeb), iftikhar.rana@seecs.edu.pk (I. Ahmad), saleemk2@lsbu.ac.uk (K. Saleem), aliz29@lsbu.ac.uk (Z. Ali).

https://doi.org/10.1016/j.bspc.2023.105803
Received 30 March 2023; Received in revised form 14 November 2023; Accepted 25 November 2023
Available online 30 November 2023
1746-8094/© 2023 The Author(s). Published by Elsevier Ltd. This is an open access article under the CC BY license (http://creativecommons.org/licenses/by/4.0/).

provides a better way to achieve the desired control objectives of high-order uncertain nonlinear systems [18,19]. Control theories have been extensively utilized for HCV treatment. To solve the optimal control problem of HCV, a fuzzy logic-based optimal control has been proposed in [20]. To decrease the viral load using ribavirin and peg-IFN-α, an optimal function for HCV dynamics has been formulated in [21]. To determine the optimal efficiency of combined ribavirin and peg-IFN-α treatment of HCV, an optimal function has also been proposed in it by taking clinical trials into account [22]. In [23], an optimal treatment program for HCV was considered that spans over 10 years. Offline optimal control method was used to carry out this work and viral load management also did not affect it. Furthermore, the controller design was based on the nominal method in which the limitation of control input was not taken into account, while the limitation of drug efficacy should be taken into account during HCV treatment. For the control of HBV infection, an adaptive nonlinear controller has been proposed in [24]. In this work, practical limitations of treatment implementation have not been considered. ANFIS-based optimal in [25] and adaptive Lyapunov-based nonlinear adaptive control method in [26] have been proposed for the control of HCV epidemic. In [27] and [28], an Adaptive Backstepping controller and modified Fractional order model have been proposed in which the limitation of drug efficacy is considered. The Basic Neumann model was used to carry out this work. Only an IFN-based treatment strategy has been utilized in this proposed control strategy while it lacked a proliferation rate of uninfected and infected hepatocytes. Using [7] model, two control inputs ribavirin and IFN have been introduced in [29] that are based on Lyapunov and fuzzy logic nonlinear controllers. Simulation results of [29] showed that infected hepatocytes and virions achieved the reference value after 30 and 55 days respectively.

To further improve the treatment time of HCV, a sliding mode-based treatment strategy for the first time has been proposed on the extended model of HCV [7] in this paper. Nonlinear sliding mode controllers (SMC) ensure global convergence and has the ability to cater for the uncertainties and external disturbance in the system model. It has advantages such as robustness against external disturbance and unpredictable parameter variations. To ensure the applicability of an SMC variant best suited for our application several SMC variants have been proposed.

In this proposed topology, drug efficacy limitation has been considered. Minimum drug quantity has been used to reduce the treatment period and the rate of SVR is also enhanced in this topology. The proposed controllers which are ISMC, DISMC, ITSMC and FOTSMC are aimed to block and reduce virions and infected hepatocytes to their required reference value. Consequently, uninfected hepatocytes will be increased to the maximum safe limit. On the basis of properties such as ripples/oscillations, overshoots/undershoots, settling time, transient time and steady-state error (SSE), all the proposed controllers have been compared with each other in the simulation result. To establish the stability of the closed-loop disease control, the Lyapunov stability theorem has been used. Two control inputs peg-IFN-α as u_1 for reducing infected hepatocytes and ribavirin as u_2 for blocking virions are used in the treatment strategies for HCV disease that are based on proposed controllers in such manners to achieve the following goals:

- During treatment, virions and infected hepatocytes are required to reduce and block to their desired reference value within 6–8 weeks.
- Uninfected hepatocytes are required to increase to their maximum steady state value T_{max}.
- Stability of the system should be ensured.

After achieving the required objectives, the treatment is stopped and blood samples of the patient are tested over the next 12 weeks. During this testing, if any viral load is not detected then the patient is wholly cured depicts that the patient further has no HCV.

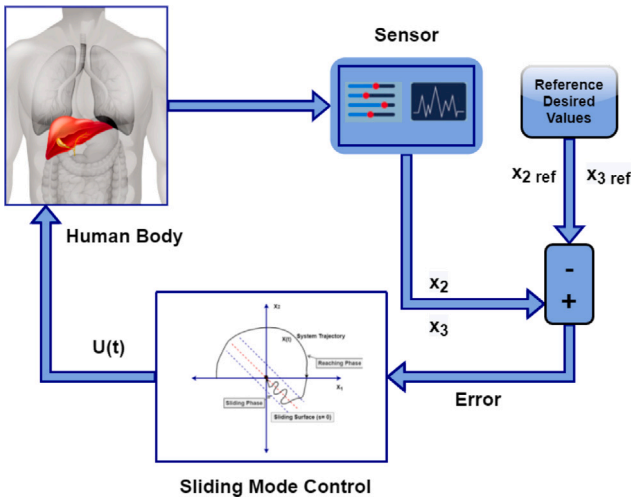

Fig. 1. Closed loop control of HCV system.

This paper has been organized as follows: In Section 2, a mathematical model of HCV has been illustrated. While in Section 3, control algorithms are depicted. In Section 4, simulation results and discussion have been presented for proposed controllers. Comparative analysis and robustness performance have been explained in Section 5. The conclusion of this work is drawn in Section 6. At the last of this document, a list of references has been given.

2. Mathematical model

Neumann et al. [3] proposed the very first mathematical model that was adopted from HIV and HBV models. Dahari had extended research work on Neumann's designed model and he considered this model as a source of hepatocytes that ignores proliferation of infected and uninfected hepatocytes ($r = 0$). Further, this model does not show any tri-phasic behavior for viral load whereas, it shows the biphasic decline of viral load under therapy. Thus, proliferation terms for both infected and uninfected hepatocytes are added in [7]. It presents the tri-phasic behavior of viral load. The first phase takes 1–4 days during which virions show abrupt decay. The second phase takes 20–30 days to virions decrease gradually further, in the third and final phases these virions are eliminated completely. To illustrate the dynamics of HCV infection, three state nonlinear mathematical HCV model is considered in this work which is suggested in [7]:

$$\begin{cases} \dfrac{dx_1}{dt} = s + r_T\, x_1 \left(1 - \dfrac{x_1 + x_2}{T_{max}}\right) - d_T\, x_1 - (1 - u_1)\beta\, x_3\, x_1 \\ \dfrac{dx_2}{dt} = (1 - u_1)\beta\, x_3\, x_1 + r_i\, x_2 \left(1 - \dfrac{x_1 + x_2}{T_{max}}\right) - \delta\, x_2 \\ \dfrac{dx_3}{dt} = (1 - u_2)\, p\, x_2 - c\, x_3 \end{cases} \tag{1}$$

Where x_1 is the amount of Uninfected Hepatocytes, x_2 is the amount of infected Hepatocytes which can prolifirate at r_T and r_i respectively. x_3 is the amount virions of HCV. The other model parameters s, d_T and T_{max} are the rate of production, death rate, and maximum concentration of Uninfected Hepatocytes, δ is the death rate of infected Hepatocytes while c and p are the production and clearance rate per virions cells.

By the combination of ribavirin, chronic HCV is treated with peg-IFN-α. Virions production is blocked by Peg-IFN-α while the treatment of de novo infection is allowed in it. Infected hepatocytes are reduced and virions production is blocked inside the patient's body using control inputs parameters u_1 and u_2. In order to make treatment realistic, the limitation of drug efficacy has been considered. It is ensured that control input values must remain between 0 and 1.

3. Control algorithms

The nonlinear nature of HCV system Eq. (1) requires the development of nonlinear algorithms that help in achieving the desired goals. This necessitates a closed-loop control model of the HCV system, which is presented in Fig. 1. To track reference levels of desired states, an error has been introduced in the system by taking the difference between states and their reference values.

There are a number of nonlinear control systems that have been developed by researchers but Sliding mode control is more viable for providing solutions for variable structures systems. It is a nonlinear control technique with high accuracy, low SSE, and robustness against model uncertainties and disturbances. It is relatively easy to implement and shows finite time convergence as compared to other nonlinear control techniques [30].The higher-order SMCs have been opted for further reducing the chattering and the SSE.

In SMC, first of all, we take a sliding surface ($S = 0$) to meet the control objectives and then formulate such control law which constrains the motion of system dynamics to this surface as shown in Fig. 2. The reach-ability condition must be satisfied for guaranteeing convergence to the sliding surface. The sliding coefficient is used to control the convergence rate of the trajectory toward the sliding surface. Chattering phenomena are observed in SMC. To reduce this chattering, a strong reachability condition is used to design the control law [31] by considering Eq. (2):

$$\dot{S}_i = -K\,|S_i|^{\alpha}\,sign\left(\frac{S_i}{\phi_i}\right) \tag{2}$$

where α is a unit between 0 and 1, $|S_i|^{\alpha}$ in the expression of $\dot{S}_i$ increases the speed of trajectory toward the sliding surface and ϕ_i is a small positive number. K is a tolerably large positive gain and $Sign$ is the Signum function which is given as follows:

$$Sign(S) = \begin{cases} -1 & if\ S < 0 \\ 0 & if\ S = 0 \\ 1 & if\ S > 0 \end{cases}$$

In SMC, control input law can be divided into two parts such as:

$$u(t) = u_{nom} + u_{sw}$$

n_{nom} is nominal SMC control law which helps the system in converging it to the equilibrium point, and n_{sw} is switching SMC control law which keeps the system trajectory on the sliding surface until its falls on the origin. The sliding surface for a general Multi Input Multi Output (MIMO) system is defined as:

$$S = [S_1, S_2 \ldots\ldots S_n]^T \tag{3}$$

S_1, S_2 up to S_n are the sliding surfaces for different outputs.

3.1. Assumptions

- Gains of the Sliding surfaces are strictly positive real numbers.
- Design coefficient k strictly positive real numbers.
- Design parameters α and ϕ are taken between 0 and 1.
- Lyapunov candidate function is a positive definite.

3.2. Integral sliding mode controller

To reduce the SSE, reject uncertainties, and reduce chattering phenomena, an integral term of errors has been introduced in the sliding surface "S_1" for infected hepatocytes and "S_2" for virions as follows:

$$\begin{cases} S_1 = a_1\,e_1 + a_2\,e_2 \\ S_2 = a_3\,e_3 + a_4\,e_4 \end{cases} \tag{4}$$

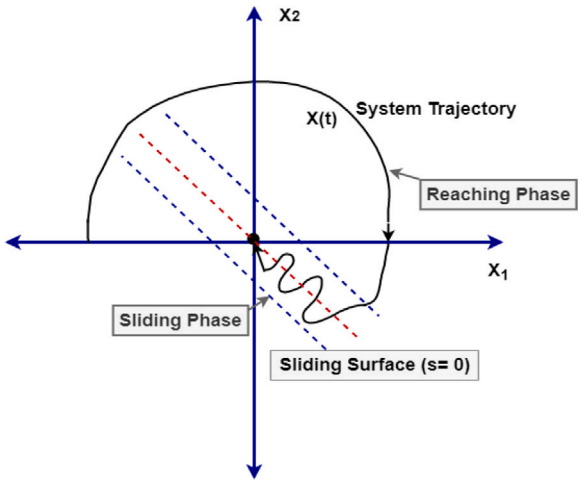

Fig. 2. Phase plane diagram of SMC.

where a_1, a_2, a_3 and a_4 are the coefficients that control the convergence rate to the sliding surface. Error e_2 is the integral of error e_1 which is the difference between infected hepatocytes and their reference value ($e_1 = x_2 - x_{2_{ref}}$). Error e_3 is the difference between the virion's state variable and its reference value ($e_3 = x_3 - x_{3_{ref}}$) while e_4 is the integral of error e_3.

Taking the time derivative of sliding surfaces given by Eq. (4) and putting $\dot{S}_1$ and $\dot{S}_2$ from Eq. (2) for $i = 1$ and 2, we get control input laws for infected hepatocytes and virions. ISMC consists of two control input laws u_{nom} and u_{sw}. Solving for control input $u_1(t)$ we get:

$$\begin{aligned} u_{nom} = \frac{1}{a_1\beta\,x_3\,x_1}\Big[& a_1\,\beta\,x_3\,x_1 + a_1\,r_i\,x_2\left(1 - \frac{x_1 + x_2}{T_{max}}\right) \\ & - a_1\,\delta\,x_2 - a_1\,\dot{x}_{2_{ref}} + a_2\,e_1\Big] \\ u_{sw} = \frac{1}{a_1\beta\,x_3\,x_1}\left[K_1\,|S_1|^{\alpha}\,sign\left(\frac{S_1}{\phi_1}\right)\right] & \end{aligned} \tag{5}$$

By combining nominal and switching SMC control law from (5) and solving for the control input $u_1(t)$:

$$\begin{aligned} u_1(t) = \frac{1}{a_1\beta\,x_3\,x_1}\Big[& a_1\,\beta\,x_3\,x_1 + K_1\,|S_1|^{\alpha}\,sign\left(\frac{S_1}{\phi_1}\right) + a_1\,r_i\,x_2 \\ & \left(1 - \frac{x_1 + x_2}{T_{max}}\right) - a_1\,\sigma\,x_2 - a_1\,\dot{x}_{2_{ref}} + a_2\,e_1\Big] \end{aligned} \tag{6}$$

Similar is the case for the control input $u_2(t)$ for the reduction of virions, the sliding manifold can be taken as:

$$\begin{aligned} u_2(t) = \left(\frac{1}{a_3\,p\,x_2}\right)\Big[& a_3\,p\,x_2 + K_2\,|S_2|^{\alpha}\,sign\left(\frac{S_2}{\phi_2}\right) \\ & - a_3\,c\,x_3 - a_3\,\dot{x}_{3_{ref}} + a_4\,e_3\Big] \end{aligned} \tag{7}$$

where

$$\begin{aligned} u_{nom} = \frac{1}{a_3\,p\,x_2}\left[a_3\,p\,x_2 - a_3\,c\,x_3 - a_3\,\dot{x}_{3_{ref}} + a_4\,e_3\right] \\ u_{sw} = \frac{1}{a_3\,p\,x_2}\left[K_2\,|S_2|^{\alpha}\,sign\left(\frac{S_2}{\phi_2}\right)\right] \end{aligned} \tag{8}$$

The control input $u_2(t)$ given by Eq. (7) is the required control input for virions to track its reference value.

Theorem 1. *Considering the system in (1), the sliding surface ($S_{1,2}$) under the assumptions given in Section 3.1, the designed proposed controller will stabilize the system provided that the condition in (2) holds. Further, in the presence of external disturbance $d(t)$, the designed controller ensures robustness.*

Proof. For stability analysis of sliding surface $S_{1,2}$, we consider the following Lyapunov candidate function as:

$$V_{1,2} = \frac{1}{2} S_1^2 + \frac{1}{2} S_2^2 \tag{9}$$

Time derivative of Eq. (9) and putting the value of $\dot{S}_1$ and $\dot{S}_2$ from Eq. (2) for $i = 1, 2$, we get

$$\begin{aligned} \dot{V}_{1,2} = S_1 \dot{S}_1 + S_2 \dot{S}_2 = S_1 \left(-K_1 |S_1|^{\alpha} sign\left(\frac{S_1}{\phi_1}\right) \right) + \\ S_2 \left(-K_2 |S_2|^{\alpha} sign\left(\frac{S_2}{\phi_2}\right) \right) \end{aligned} \tag{10}$$

Eq. (57) for i= 1 and 2 from Eq. (33) becomes:

$$\begin{aligned} \dot{V}_{1,2} &= -K_1 |S_1|^{\alpha} \phi_1 \left| \frac{S_1}{\phi_1} \right| - K_2 |S_2|^{\alpha} \phi_2 \left| \frac{S_2}{\phi_2} \right| \\ &= -K_1 |S_1|^{\alpha} \phi_1 \frac{|S_1|}{\phi_1} - K_2 |S_2|^{\alpha} \phi_2 \frac{|S_2|}{\phi_2} \end{aligned} \tag{11}$$

$|\phi_1| = \phi_1$, $|\phi_2| = \phi$ and $\phi_{1,2} > 0$, we have:

$$\dot{V}_{1,2} = -K_1 |S_1|^{\alpha_1 + 1} - K_2 |S_2|^{\alpha_2 + 1} \tag{12}$$

Eq. (12) shows that $\dot{V}_{1,2} < 0$, thus making the system stable by using Lyapunov theory.

3.3. Double integral sliding mode controller

The second integral has been added to the sliding surface to compensate remaining SSE and mitigate the chattering. Consider the following sliding surfaces:

$$\begin{aligned} S_3 &= a_5 e_1 + a_6 e_2 + a_7 e_5 \\ S_4 &= a_8 e_3 + a_9 e_4 + a_{10} e_6 \end{aligned} \tag{13}$$

where a_5, a_6, a_7, a_8, a_9 and a_{10} are coefficients of the sliding surface. e_2 is the integral error of e_1. e_5 is the double integral error of the infected hepatocytes state error e_1. e_3 is the error between the virions and their reference value $x_{3_{ref}}$, e_4 is its integral and e_6 is its double integral.

In mathematical form, errors are expressed as:

$$e_1 = x_2 - x_{2_{ref}} \tag{14}$$

$$e_2 = \int \left(x_2 - x_{2_{ref}} \right) dt \tag{15}$$

$$e_5 = \int \left\{ \int \left(x_2 - x_{2_{ref}} \right) dt \right\} dt \tag{16}$$

Now time derivative of the sliding surface S_i for $i = 3, 4$ to get the control inputs for infected hepatocytes and virions. Solving for the control input u_1, we get:

$$\begin{aligned} u_1(t) = \left(\frac{1}{a_5 \beta x_3 x_1} \right) \Bigg[a_5 \beta x_3 x_1 + K_3 |S_3|^{\alpha} sign\left(\frac{S_3}{\phi_3}\right) \\ + a_5 r_i x_2 \left(1 - \frac{x_1 + x_2}{T_{max}}\right) - a_5 \delta x_2 - a_5 \dot{x}_{2_{ref}} + \\ a_6 e_1 + a_7 e_2 \Bigg] \end{aligned} \tag{17}$$

Computing for control input $u_2(t)$ used for the blocking and reduction of virions from HCV dynamics system will be:

$$\begin{aligned} u_2(t) = \left(\frac{1}{a_8 p x_2} \right) \Bigg[a_8 p x_2 + K_4 |S_4|^{\alpha} sign\left(\frac{S_4}{\phi_4}\right) - a_8 c x_3 \\ - a_8 \dot{x}_{2_{ref}} + a_9 e_4 + a_{10} e_6 \Bigg] \end{aligned} \tag{18}$$

Theorem 2. *Considering the system in (1), the sliding surface ($S_{3,4}$) under the assumptions given in Section 3.1, the designed proposed controller will stabilize the system provided that the condition in (2) holds. Further, in the presence of external disturbance $d(t)$, the designed controller ensures robustness.*

Proof. For stability analysis of sliding surface $S_{3,4}$, we consider the following Lyapunov candidate function as:

$$V_{3,4} = \frac{1}{2} S_3^2 + \frac{1}{2} S_4^2 \tag{19}$$

By taking time derivative of Eq. (19) and substituting $\dot{S}_3$ and $\dot{S}_4$ from Eq. (2) for $i = 3, 4$ yields:

$$\begin{aligned} \dot{V}_{3,4} = S_3 \dot{S}_3 + S_4 \dot{S}_4 = S_3 \left(-K_3 |S_3|^{\alpha} sign\left(\frac{S_3}{\phi_3}\right) \right) + \\ S_4 \left(-K_4 |S_4|^{\alpha} sign\left(\frac{S_4}{\phi_4}\right) \right) \end{aligned} \tag{20}$$

Eq. (20) for i = 3 and 4 becomes:

$$\begin{aligned} \dot{V}_{3,4} &= -K_3 |S_3|^{\alpha} \phi_3 \left| \frac{S_3}{\phi_3} \right| - K_4 |S_4|^{\alpha} \phi_4 \left| \frac{S_4}{\phi_4} \right| \\ &= -K_3 |S_3|^{\alpha} \phi_3 \frac{|S_3|}{\phi_3} - K_4 |S_4|^{\alpha} \phi_4 \frac{|S_4|}{\phi_4} \end{aligned} \tag{21}$$

$|\phi_3| = \phi_3$, $|\phi_4| = \phi$ and $\phi_{3,4} > 0$, we have:

$$\dot{V}_{3,4} = -K_3 |S_3|^{\alpha_3 + 1} - K_4 |S_4|^{\alpha_4 + 1} \tag{22}$$

As the derivative of Lyapunov candidate function $\dot{V}_{3,4}$ given by Eq. (22) is negative definite, the system is stable.

3.4. Integral terminal sliding mode controller (ITSMC)

In order to eliminate the singularity problem and to achieve high state accuracy tracking, Integral terminal SMC has been proposed. Defining the ITSMC sliding surface as follows:

$$S_5 = e_1 + \kappa_5 \left[\int_0^t e_1 \, dt \right]^{\lambda_5} \tag{23}$$

where κ_5 is design parameter of sliding manifold, λ_5 is positive number such that $1 < \lambda_5 < 2$. e_1 is the tracking error variable between infected hepatocytes. Time derivative of the sliding surface and Substituting $\dot{S}_5$ and solving for the control input $u_1(t)$, we get

$$\begin{aligned} u_1(t) = \left(\frac{1}{\beta x_3 x_1} \right) \Bigg[K_5 |S_5|^{\alpha} sign\left(\frac{S_5}{\phi_5}\right) + \beta x_3 x_1 + \\ r_i \left(1 - \frac{x_1 + x_2}{T_{max}}\right) - \delta x_2 - \dot{x}_{2_{ref}} + \\ \kappa_5 (\lambda_5) e_1 \left[\int_0^t e_1 \, dt \right]^{\lambda_5 - 1} \Bigg] \end{aligned} \tag{24}$$

Similarly for the state variable x_3, the sliding surface S_6 is taken as:

$$S_6 = e_2 + \kappa_6 \left[\int_0^t e_8 \, dt \right]^{\lambda_6} \tag{25}$$

where e_2 is the tracking error variable between the virions and their reference value. Time derivative of Eq. (25) and solving for control input $u_2(t)$, we get

$$\begin{aligned} u_2(t) = \left(\frac{1}{p x_2} \right) \Bigg[-K_6 |S_6|^{\alpha} sign\left(\frac{S_6}{\phi_6}\right) + p x_2 - c x_3 - \dot{x}_{3_{ref}} + \\ \kappa_6 (\lambda_6) e_2 \left[\int_0^t e_2 \, dt \right]^{\lambda_6 - 1} \Bigg] \end{aligned} \tag{26}$$

Theorem 3. *Considering the system in (1), the sliding surface ($S_{3,4}$) under the assumptions given in Section 3.1, the designed proposed controller will stabilize the system provided that the condition $\dot{S}_5 = -K |S_5|^{\alpha} sign\left(\frac{S_5}{\phi_5}\right)$ and $\dot{S}_6 = -K |S_6|^{\alpha} sign\left(\frac{S_6}{\phi_6}\right)$ holds. Further, in the presence of external disturbance $d(t)$, the designed controller ensures robustness.*

Proof. For the stability of sliding manifolds S_5 and S_6, taking Lyapunov candidate function as:

$$V_{5,6} = \frac{1}{2}S_5^2 + \frac{1}{2}S_6^2 \tag{27}$$

By taking time derivative of Eq. (27) yields:

$$\dot{V}_{5,6} = S_5\dot{S}_5 + S_6\dot{S}_6 \tag{28}$$

Putting $\dot{S}_5$ and $\dot{S}_6$ in Eq. (28) gives:

$$\dot{V}_{5,6} = -S_5\left(K_5\,|S_5|^{\alpha}\,sign(\frac{S_5}{\phi_5})\right) - S_6\left(K_6\,|S_6|^{\alpha}\,sign(\frac{S_6}{\phi_6})\right) \tag{29}$$

As the derivative of Lyapunov candidate function $\dot{V}_{5,6}$ by Eq. (41) is negative definite for κ_5 and κ_6 greater than zero, the system is stable.

3.5. Fractional order terminal sliding mode controller (FOTSMC)

The main purpose of this study is to design a stable control strategy for HCV under IFN and Ribavirin therapy based on Fractional Order Control (FOC). FOC has been implemented for the HCV system with a combination of Terminal Sliding mode control (TSMC). The concept of such a method is to develop a sliding surface which is the fusion of FOC with TSMC characteristics. The main advantage of FOTSMC with the terminal sliding surface using fractional order derivative calculus is avoiding singularity issues and faster convergence speed compared to conventional ITSMC. FOTSMC control laws are developed to ensure the finite time convergence of HCV system states to their reference level based on the Lyapunov stability theorem.

FOTSMC sliding surface is proposed and given by:

$$S_7 = c_5D^{-\alpha}e_1 + c_6D^{\alpha}|e_1|^{\gamma}sgn(e_1) \tag{30}$$

where c_5, c_6 and γ are positive numbers. D is fractional operator and defined as:

${}_a\mathbb{D}_t^{\alpha}$ is fundamental fractional operator defined as:

$${}_a\mathbb{D}_t^{\alpha} = \begin{cases} \frac{d^{\alpha}}{dt^{\alpha}} & \mathbb{R}(\alpha) > 0 \\ 1, & R(\alpha) = 0 \\ \int_a^t (d\tau)^{-\alpha}, & R(\alpha) < 0 \end{cases} \tag{31}$$

where $R(\alpha)$ is real set number and α represent fractional operator order [32]. The fractional operator is defined by many definitions such as:

Definition 1. Riemann–Liouville fractional integral and derivative αth order of the function $f(t)$ w.r.t time is:

$${}_a\mathbb{D}_t^{\alpha} = \frac{d^{\alpha}}{dt^{\alpha}}f(t) = \frac{1}{\Gamma(m-\alpha)}\frac{d^m}{dt^m}\int_{\alpha}^{t}\frac{f(\tau)}{(t-\tau)^{\alpha-m+1}}d\tau \tag{32}$$

$${}_a\mathbb{D}_t^{-\alpha} = I^{\alpha}f(t) = \frac{1}{\Gamma(\alpha)}\int_{\alpha}^{t}\frac{f(\tau)}{(t-\tau)^{1-\alpha}}d\tau \tag{33}$$

where "m" is first integer and larger than "a" such as $m-1 < \alpha < m, t-\alpha$ is interval integration.

Definition 2. Caputo fractional integral and derivative αth order of the function $f(t)$ w.r.t time is [32]:

$${}_a\mathbb{D}_t^{\alpha} = \begin{cases} \frac{1}{\Gamma(\upsilon-\alpha)}\int_{\alpha}^{t}\frac{f^{\upsilon}(\tau)}{(t-\tau)^{\alpha-\upsilon+1}}d\tau \\ (\upsilon-1 \le \alpha < \upsilon) \\ \frac{d^m}{dt^n}f(t)(\alpha = \upsilon) \end{cases} \tag{34}$$

Definition 3. Order α GL definition is defined as [32]:

$${}^{GL}_{a}\mathbb{D}_t^{\alpha}f(t) = \lim_{ts\to 0}\frac{1}{ts^{\alpha}}\sum_{j=0}^{\frac{(t-\alpha)}{h}}(-1)^j\binom{\alpha}{j}f(t-jh) \tag{35}$$

$$\binom{\alpha}{j} = \frac{\Gamma(\alpha+1)}{\Gamma(j+1)\Gamma(\alpha-j+1)} \tag{36}$$

Where the time step is represented by ts and the gamma function by $\Gamma(.)$. The stability of non-integer systems has been thoroughly discussed in the literature [33,34]. The Oustaloup recursive approximation algorithm [35] is used to approximate fractional orders using a classical integer order transfer function.

e_1 is tracking error variable between the infected hepatocytes and their reference value given as:

$$e_1 = x_2 - x_{2_{ref}} \tag{37}$$

The time derivative of the sliding manifold is

$$\dot{S}_7 = c_5D^{1-\alpha}e_1 + c_6\gamma D^{\alpha}\underbrace{D^1|e_1|^{\gamma}sgn(e_1)}$$

$$\dot{S}_7 = c_5D^{1-\alpha}e_1 + c_6\gamma D^{\alpha}|e_1|^{\gamma-1}\dot{e}_1 \tag{38}$$

Applying $D^{-\alpha}$ to both side of Eq. (38), yields:

$$D^{1-\alpha}\dot{S}_7 = c_5D^{1-2\alpha}e_1 + c_6\gamma|e_1|^{\gamma-1}\dot{e}_1 \tag{39}$$

$D^{1-\alpha}$ represent fractional derivative term. For simplicity, we can represent it as $D^{\hat{\alpha}}$. Convenient form of Eq. (39) is written as:

$$D^{\hat{\alpha}}\dot{S}_7 = c_5D^{1-2\alpha}e_1 + c_6\gamma|e_1|^{\gamma-1}\dot{e}_1 \tag{40}$$

Taking time derivative of Eq. (37) and putting it in Eq. (40), we have:

$$D^{\hat{\alpha}}\dot{S}_7 = c_5D^{1-2\alpha}e_1 + c_6\gamma|e_1|^{\gamma-1}\left((1-u_1)\beta\,x_3\,x_1 + r_i\,x_2(1-\frac{x_1+x_2}{T_{max}}) - \delta\,x_2 - \dot{x}_{2_{ref}}\right) \tag{41}$$

Solving Eq. (41) for control input $u_1(t)$, we get:

$$u_1(t) = u_{sw} + u_{nom} \tag{42}$$

$$u_{norm} = \frac{1}{\beta\,x_3\,x_1}\left[r_i\,x_2(1-\frac{x_1+x_2}{T_{max}}) - \delta\,x_2 - \dot{x}_{2_{ref}} - \frac{c_5|e_1|^{1-\gamma}}{\gamma c_6}D^{1-2\alpha}(e_1) + \beta\,x_3\,x_1\right] \tag{43}$$

$$u_{sw} = \frac{1}{\beta\,x_3\,x_1}|e_s|^{1-\gamma}\left[-\frac{k_{r_3}}{\gamma c_6}sgn(S_7)\right] \tag{44}$$

Similarly for the state variable x_3, the sliding surface S_8 is taken as:

$$S_8 = c_7D^{-\alpha}e_2 + c_8D^{\alpha}|e_2|^{\gamma}sgn(e_2) \tag{45}$$

where e_2 is the tracking error variable between the virions and their reference value expressed as:

$$e_2 = x_3 - x_{3_{ref}} \tag{46}$$

Taking time derivative of the surface given in Eq. (45) and putting the values of $\dot{e}_2$, one gets:

$$D^{\hat{\alpha}}\dot{S}_8 = c_7D^{1-2\alpha}e_2 + c_8\gamma|e_2|^{\gamma-1}\left[(1-u_2)\,p\,x_2 - c\,x_3 - \dot{x}_{3_{ref}}\right] \tag{47}$$

Solving the above equation for $u_2(t)$ one gets:

$$u_2(t) = u_{norm}(t) + u_{sw}(t) \tag{48}$$

$$u_{norm}(t) = 1 + \frac{1}{p\,x_2}\left[p\,x_2 - c\,x_3 - \dot{x}_{3_{ref}} - \frac{c_7|e_{10}|^{1-\gamma}}{\gamma c_8}D^{1-2\alpha}(e_2)\right] \tag{49}$$

$$u_{sw} = \frac{1}{p\,x_2}|e_{10}|^{1-\gamma} - \frac{k_{r4}}{\gamma c_7}(sgn(S_7)) \tag{50}$$

The closed-loop stability of the proposed control paradigm is achieved using the Lyapunov stability theorem selected as $V_i = \frac{1}{2}S_i^2$. A fractional operator $D^{\bar{\alpha}}$ is applied to the Lyapunov function V_i resulting in the following expression.

$$D^{\bar{\alpha}}V_1 \leq S_i D^{\bar{\alpha}} S_i + \sum_{j=1}^{\infty} \frac{\mathcal{T}(1+\bar{\alpha})}{\mathcal{T}(1+\bar{\alpha}-j)(1+\mathrm{j})} D^{\mathrm{j}} S_i D^{\bar{\alpha}-j} S_i \tag{51}$$

Consider the following inequality:

$$\sum_{j=1}^{\infty} \frac{T(1+\bar{\alpha})}{\mathcal{T}(1+\bar{\alpha}-j)(1+\mathrm{j})} D^{\mathrm{i}S_i} D^{\bar{\alpha}-j} S_i \leq \rho \left|S_i\right| \tag{52}$$

Further simplification

$$D^{\bar{\alpha}}V_i \leq S_i D^{\bar{\alpha}} S_i + \lambda_3 \left|S_i\right| \tag{53}$$

$$\begin{aligned} D^{\bar{\alpha}}V_1 \leq & \left\{c_5 D^{1-2\alpha} e_1 + c_6 \gamma |e_1|^{\gamma-1} \right. \\ & \left. \left((1-u_1)\beta\, x_3\, x_1 + r_i\, x_2\, (1 - \frac{x_1 + x_2}{T_{max}}) - \delta\, x_2 - \dot{x}_{2_{ref}}\right)\right\} \\ & + \lambda_{31} \left|S_7\right| \end{aligned} \tag{54}$$

$$\begin{aligned} D^{\bar{\alpha}}V_2 \leq & \left\{c_7 D^{1-2\alpha} e_2 + c_8 \gamma |e_{10}|^{\gamma-1} \right. \\ & \left. \left((1-u_2)\, p\, x_2 - \, c\, x_3 - \dot{x}_{3_{ref}}\right)\right\} + \lambda_{32} \left|S_8\right| \end{aligned} \tag{55}$$

Finally, the simplification, obtain:

$$D^{\bar{\alpha}}V_i \leq -\lambda_i |S_i| + \rho |S_i| \tag{56}$$

By choosing λ_i, such that $\lambda_i\ |S_i| > \rho |S_i|$, then the expression $D^{\bar{\alpha}}V_i$ is always negative.

Theorem 4. *Using Lyapunov stability theorem, consider fractional order sliding surfaces (30) and (45), it guarantees that fractional order sliding surface is stable and converge to zero.*

$$\begin{aligned} S_7 + S_8 = & \left[c_5 D^{-\alpha} e_1 + c_6 D^{\alpha} |e_1|^{\gamma} sgn(e_1)\right] + \\ & \left[c_7 D^{-\alpha} e_2 + c_8 D^{\alpha} |e_2|^{\gamma} sgn(e_2)\right] = 0 \end{aligned} \tag{57}$$

Consider the fractional error dynamics as:

$${}_a\mathbb{D}_t^{\alpha} e_1 + {}_a\mathbb{D}_t^{\alpha} e_2 = -\lambda_1 e_1 - \lambda_2 e_2 \quad 0 < \alpha < 1. \tag{58}$$

Considering the Lyapunov function for both errors, as follows:

$$V_{e_1,e_2} = \frac{1}{2}e_1^2 + \frac{1}{2}e_2^2 \tag{59}$$

Taking fractional derivatives on both sides, one has:

$$\begin{aligned} {}_a\mathbb{D}_t^{\alpha} V_{e_1,e_2} = & \frac{1}{2}\, {}_a\mathbb{D}_t^{\alpha}\, e_1^2 + \frac{1}{2} {}_a\mathbb{D}_t^{\alpha}\, e_2^2 \\ \leq e_1\, {}_a\mathbb{D}_t^{\alpha}\, e_1 + e_2\, {}_a\mathbb{D}_t^{\alpha}\, e_2 = & -\lambda_1\, e_1^2 - \lambda_2\, e_2^2. \end{aligned} \tag{60}$$

It implies that the stability of the system is guaranteed.

4. Simulation results and comparison

In this section, the performance of the proposed control input laws Eqs. (6) and (7) for ISMC, by Eqs. (17) and (18) for DISMC, by Eqs. (24) and (26) for ITSMC, by Eqs. (42) and (48) for FOTSMC has been presented through the simulation results using MATLAB/Simulink being simulated for the time period of 50 days. The initial value of the infected hepatocytes is recorded as 50,000 IU/L. The initial value of the uninfected hepatocytes is recorded as 555 IU/L while for virions it is 20,000 IU/L. The Polymerase Chain Reaction (PCR) calculates these values. HCV RNA viruses are found by the HCV RNA PCR blood test. In order to reach the accepted condition at the equilibrium point of $x = [8000000, 0, 0]^T$, the control was applied for regulating virions, infected hepatocytes, and uninfected hepatocytes. The initial condition of the error dynamics influences the reachability time of the states to a desired reference level. By setting a high value as the initial condition for the double integral's reachability time, the time required can be significantly reduced. However, this approach initiates the chemotherapy process with a high-dose injection, which is not ideal. In the proposed control strategy, a gradual initiation of the chemotherapy dose has been implemented by setting the initial condition of error dynamics to zero. The initial condition for the error dynamics in each proposed controller's case is $e_i = 0$. The required reference values for virions, infected hepatocytes, and uninfected hepatocytes were set at $x_{3_{ref}} = 0$, $x_{2_{ref}} = 0$, $T_{max} = 8{,}000{,}000$, respectively. HCV dynamical model used all parametric values from [36] which are enlisted here. Design parameters for the proposed controllers are obtained by trial and error method. Appropriate desired reference value can be achieved by changing the gain value. Nonlinear HCV system parameters and values are given as:

- $p = 20$, $c = 10$, $\beta = 10^{-7}$, $s = 0.0024 * 10^{-7}$.
- $r_T = 2$, $r_i = 1$, $d_T = 0.003$, $\delta = 0.2$.

For ISMC, gains parameters values are defined as:

- $a_1 = 9780$, $a_2 = 4$, $a_3 = 1$, $a_4 = 1$.
- $K_1 = 6300$, $K_2 = 35{,}000$
- $\alpha = 0.5$, $\phi_1 = \phi_2 = 0.5$

DISMC gain parameters values are as follows:

- $a_5 = 9000$, $a_6 = 1$, $a_7 = 12{,}590{,}000$, $a_8 = 7500$, $a_9 = 1$, $a_{10} = 90{,}000$
- $K_3 = 65{,}000$, $K_4 = 65{,}000$
- $\alpha = 0.5$, $\phi_3 = \phi_4 = 0.5$

ITSMC gain parameter values are as follows:

- $\lambda_5 = 1.5$, $\lambda_6 = 1.5$
- $\kappa_5 = 6500$, $\kappa_6 = 90{,}000$
- $\alpha = 0.5$, $\phi_5 = \phi_6 = 0.5$

Similarly, for FOTSMC:

- $c_5 = 0.15$, $c_6 = 0.01$, $c_7 = 0.20$, $c_8 = 0.0010$
- $K_{r_3} = 0.050$, $K_{r_4} = 0.0001$
- $\gamma = 1.5$, $\alpha = 0.5$, $\phi_3 = \phi_4 = 0.5$

The uncontrolled behavior (without drug usage) of the system is shown by Fig. 3. In the disease's early stage, infected hepatocytes and virions grow rapidly due to which uninfected hepatocytes decrease. However, using the proposed controllers ISMC, DISMC, ITSMC and FOTSMC for the drug injection, the concentration of the virions and infected hepatocytes decreases and is tracked to its reference value.

After exposure to the virus during the first phase of the disease, the drug efficacy u_1 must be at the highest level for a shorter time period on the basis of control inputs. Later, when a certain level for the second phase is achieved, the drug efficacy decreases and it remains at the lowest level for the rest of the treatment period. Moreover, the drug efficacy u_2 remains lower in the first phase and it reaches a higher level in the second phase gradually. To keep the drug amount within safe limits, the maximum value for the drug efficacy u_1 and u_2 is set to be 0.96.

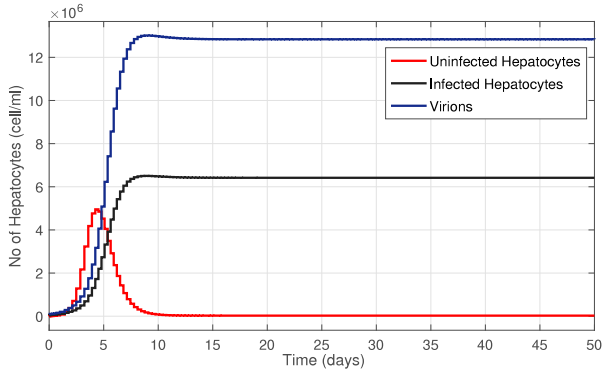

Fig. 3. Uncontrolled response of all states of HCV.

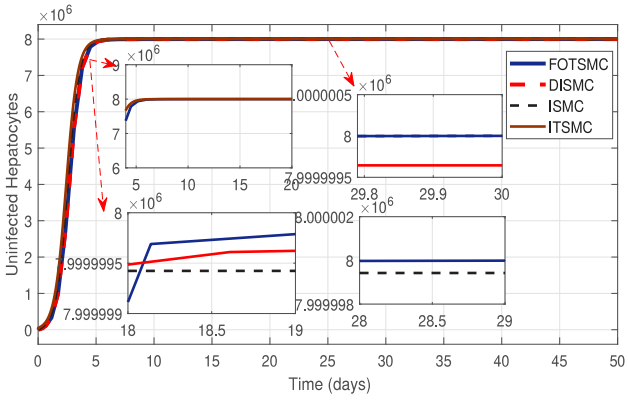

Fig. 4. Behavior of uninfected hepatocytes.

This section consists of four subsections. The first subsection shows the response of Uninfected Hepatocytes for drug injection with proposed controllers. Similarly, the second and third subsection shows the behavior of Infected Hepatocytes and Virions respectively. In the fourth subsection, all the proposed controllers have been compared with each other on the basis of transient response, SSE, undershoot/overshoot, ripples and chattering in their performances for the control and reduction of HCV.

4.1. Response of Uninfected Hepatocytes

Here the Response of Uninfected Hepatocytes state of HCV with all proposed controllers have been made. Fig. 4 shows the behavior of uninfected hepatocytes with drug injection. Uninfected hepatocytes show a remarkable increase and achieve T_{max} which is the maximum concentration of uninfected hepatocytes in the liver and its value is 8,000,000 IU/L. Uninfected Hepatocytes transient time takes the same time with ISMC and FOTSMC to T_{max}. SSE has been observed in the uninfected hepatocytes with the ISMC. FOTSMC shows no SEE in achieving T_{max} limit. Using FOTSMC, uninfected hepatocytes achieve T_{max} rapidly with no SSE than that using DISMC. ITSMC shows good tracking of uninfected hepatocytes to T_{max} with better transient time and no SSE. The control inputs u_1 and u_2 for ISMC has been shown in Fig. 5.

4.2. Response of Infected Hepatocytes

Fig. 6 shows the behavior of the infected hepatocytes under the proposed controllers which shows that their tracking time to the reference values is very fast with ISMC as compared to that of FOTSMC. However, ISMC observes huge SSE in tracking the reference value. The infected

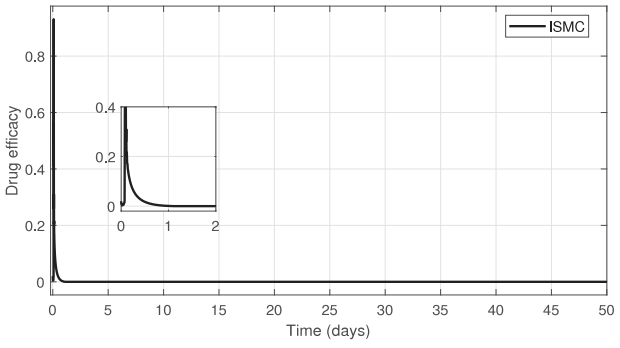

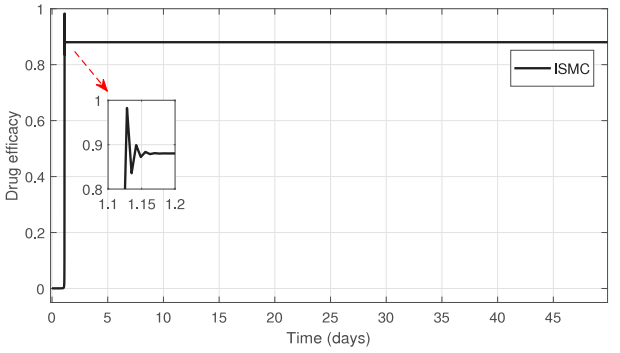

Fig. 5. (a) Control input u_1 for ISMC (b) Control input u_2 for ISMC.

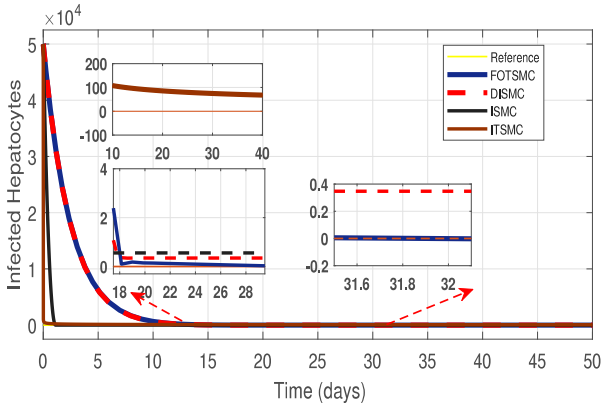

Fig. 6. Behavior of infected hepatocytes.

hepatocytes track the reference value in almost 18 days having zero SSE by using FOTSMC (as clear from the zoomed portion of the graph).

The tracking behavior of the infected hepatocytes is slightly better with DISMC than that with FOTSMC. Using antiviral drugs with DISMC, infected hepatocytes are tracked to their reference level in 17 days while they take 18 days with FOTSMC. But again DISMC shows a small SSE while it tracked nicely with FOTSMC having no SSE to its reference level. ITSMC shows tracking to reference level having SSE as well. FOTSMC shows better behavior for tracking infected hepatocytes. The control inputs u_1 and u_2 for DISMC has been shown in Fig. 7. The maximum starting value of the interferon for the adults infected with HCV genotype 1 (weight > 75 kg) is 180 micrograms (mcg/mL). With interferon, the maximum dose for the ribavirin given to the patient is 1000–1200 mg/d.

4.3. Response of virions

The behavior of the virions of the HCV is shown in Fig. 8. They approach the reference value very fast with the ISMC as compared to

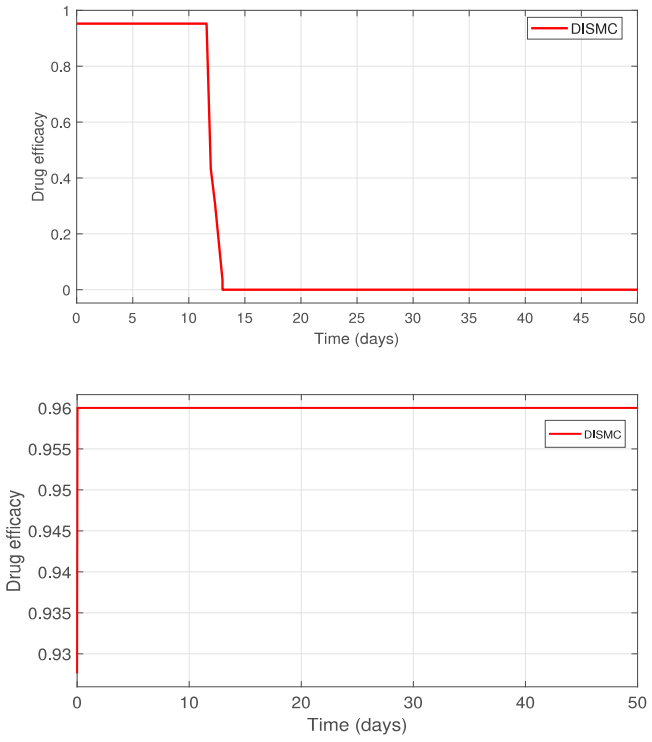

Fig. 7. (a) DISMC control input u_1 (b) DISMC control input u_2.

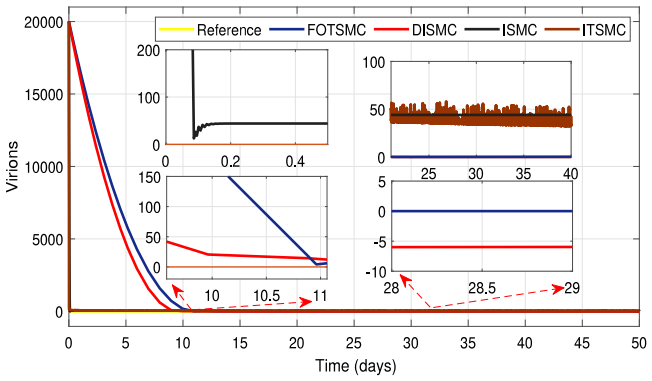

Fig. 8. Behavior of Virions.

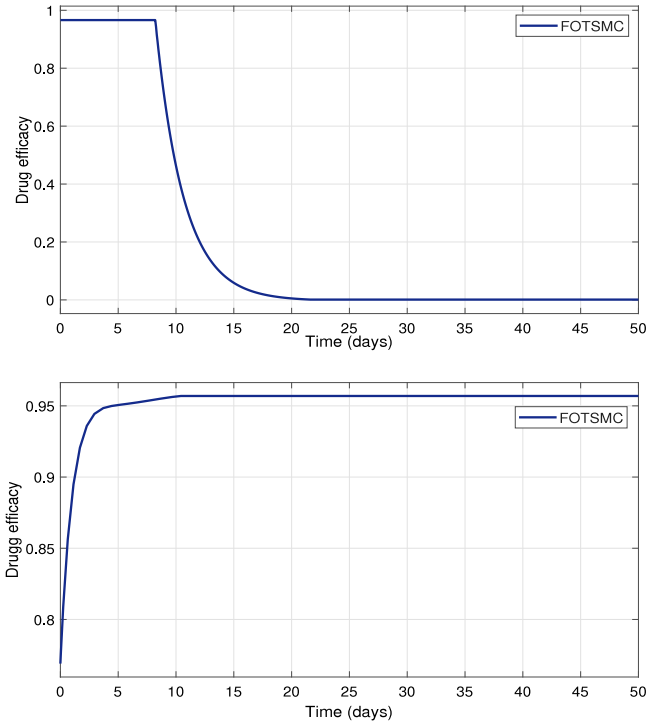

Fig. 9. (a) FOTSMC control input u_1 (b) FOTSMC control input u_2.

Table 1
Response of proposed controllers.

Uninfected hepatocytes				
Response	ISMC	DISMC	FOTSMC	ITSMC
SSE (cells)	100	0.4	0	0
Overshoot/Undershoot	0	0	0	0
Settling time (day)	8	21	10	8
Converging time (day)	5	5.1	5	5
Infected hepatocytes				
Response	ISMC	DISMC	FOTSMC	ITSMC
SSE (cells)	0.6	6	0	60
Overshoot/Undershoot	0	0	0	0
Settling time (days)	0.8	9	9	40
Converging time (days)	1	10	10	10
Virions				
Response	ISMC	DISMC	FOTSMC	ITSMC
SSE (cells)	45	6	0	50
Overshoot/Undershoot	0	0	0	0
Settling time (days)	0.3	8	9	45
Converging time (days)	0.5	9	10	0.3

that of FOTSMC. However, the ISMC gives a large SSE of about 45 hepatocytes while tracking the reference value. The tracking time of virions with the FOTSMC is 10 days of the treatment using peg-IFN-α as u_1 and ribavirin as u_2 while virions track to zero with no SSE.

Fig. 8 shows that the virions track to the reference faster by using ITSMC but with SSE and chattering. FOTSMC again shows no SSE in tracking the reference of virions and completely eliminates the virions. The control inputs u_1 and u_2 for FOTSMC has been shown in Fig. 9.

4.4. Discussion

The performance of ISMC, DISMC, ITSMC and FOTSMC have been compared with each other. The comparison of proposed controllers is based on controller characteristics such as overshoot, undershoot, SSE, transient, settling time, and chattering while converging to the reference level and the settling time. Uninfected hepatocytes converge to the maximum level T_{max} in just 5 days. Settling time is about 10 days with no SSE. Tracking of infected hepatocytes and virions to their reference level having no SSE is done in 10 days with FOTSMC.

SSE has been observed in all the states of the HCV using DISMC. It is 0.4 hepatocytes below T_{max} level, 0.4 and 6 hepatocytes below the reference level of infected hepatocytes and virions respectively. The transient time for uninfected hepatocytes with DISMC is 5.1 days while settling time is 21 days. The convergence time for virions is 9 days and for infected hepatocytes, it is 10 days.

ISMC provides better convergence behavior than all the other proposed controllers but observes not negligible SEE. It takes 5 days to approach the T_{max} and the settling time is 8 days for uninfected hepatocytes, 1 day for the infected hepatocytes and half a day for virions. But it gives an SSE of 0.1 IU/L, 0.6 IU/L and 45 IU/L hepatocytes in uninfected hepatocytes, infected hepatocytes and virions respectively.

With ITSMC, the transient time and settling time of uninfected hepatocytes maximum level T_{max} is 4 and 8 days respectively with no SSE. The infected hepatocytes and virions track the reference in almost half day with SSE and chattering with ITSMC.

In ISMC, the integral term in the control law is used to mitigate the SSE. However, SSE values of Uninfected Hepatocytes, Infected Hepatocytes, and virions respectively as 100, 0.6, and 45 cells indicate that ISMC helps in reducing the error but does not entirely eliminate and thus, the residual steady-state error persists. The DISMC extends the integral action to double integral, thereby enhancing the controller's ability to eliminate SSE as shown in Table 1. DISMC signifies a significant reduction in SSE as compared to ISMC, yet a finite residual error remains in all states. The most notable result is the elimination of SSE in all states employing FOTSMC and this is due to the use of fractional calculus which allows for a more accurate representation of system dynamics. Fractional order systems inherently exhibit smoother transitions between states compared to their integer-order counterparts, and this can contribute to a smooth transition, continuous control signals, and improved accuracy. The zero SSE showed the efficacy of fractional order dynamics in achieving precise tracking without any persistent deviation from the desired reference state.

ISMC provides relatively fast convergence for infected Hepatocytes and virions but may exhibit delays in settling time for Uninfected Hepatocytes. ITSMC excels in achieving rapid convergence for the virions, showing the effectiveness of the terminal condition in controlling this specific state. FOTSMC, while maintaining a comparable settling time for Uninfected Hepatocytes, demonstrates faster convergence for Infected Hepatocytes and the virions, emphasizing the benefits of fractional order dynamics. So, FOTMSC performs better than other proposed controllers in terms of SSE, overshoot, transient, and settling times. It gives better performance in blocking and tracking of infected hepatocytes and virions.

5. Proof of robustness

External disturbance, initial conditions, and parametric variation have been simulated to test the robustness of the proposed controllers ISMC, DISMC, ITSMC and FOTSMC. The results are presented below:

5.1. Effect of external disturbance/noise

White noise having a magnitude of 10% has been introduced into output values in order to evaluate the efficacy of the proposed treatment strategy under measurement noise. Eq. (1) has been presented in the presence of white noise, given by;

$$\begin{cases} \dfrac{dx_1}{dt} = s + r_T x_1(1 - \dfrac{x_1 + x_2}{T_{max}}) - d_T x_1 - (1-u_1)\beta x_3 x_1 + v_k \\ \dfrac{dx_2}{dt} = (1-u_1)\beta\, x_3\, x_1 + r_i\, x_2 (1 - \dfrac{x_1 + x_2}{T_{max}}) - \delta\, x_2 + v_k \\ \dfrac{dx_3}{dt} = (1-u_2)\, p\, x_2 - c\, x_3 + v_k \end{cases} \tag{61}$$

The comparative analysis of all proposed nonlinear controllers in the presence of noise has been shown in Fig. 10 for uninfected hepatocytes, Fig. 12 and Fig. 11 for virions and infected hepatocytes respectively. ITSMC and FOTSMC can withstand such a level of noise and converge all states to their reference values with acceptable performance. Only the ISMC displays a very noisy output. FOTSMC controller is the best due to its fast convergence with reduced SSE and chattering among all the proposed controllers. The main reason behind FOTSMC exhibits improved robustness to uncertainties and disturbances. This enhanced robustness helps maintain stability without the need for aggressive control actions that contribute to chattering and SSE.

5.2. Effect of different initial conditions

Figs. 13, 14 and 15 show the behavior of uninfected hepatocytes, infected hepatocytes and virions with different initial conditions using FOTSMC. Using the values of gains, FOTSMC performs better for tracking all the states.

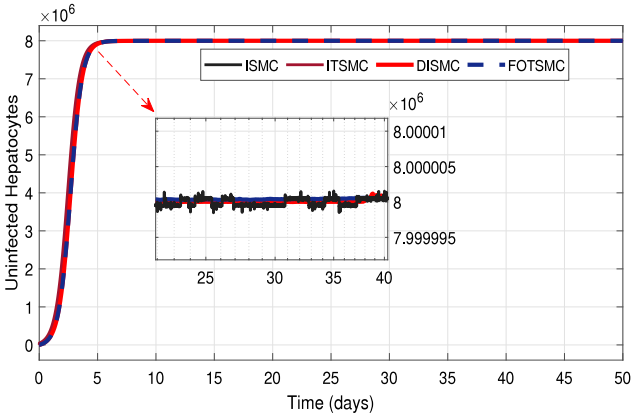

Fig. 10. Behavior of uninfected hepatocytes in the presence of noise.

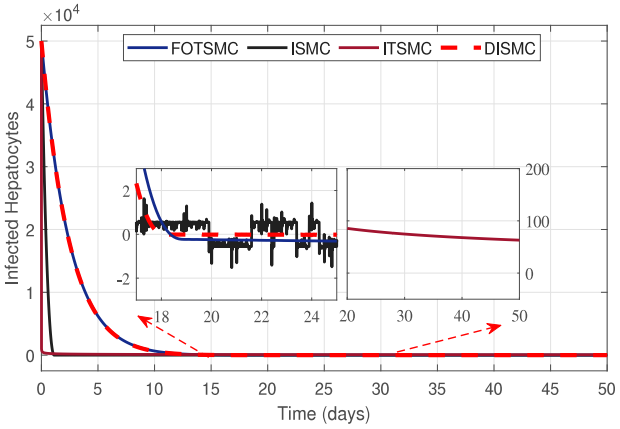

Fig. 11. Behavior of infected hepatocytes in the presence of noise.

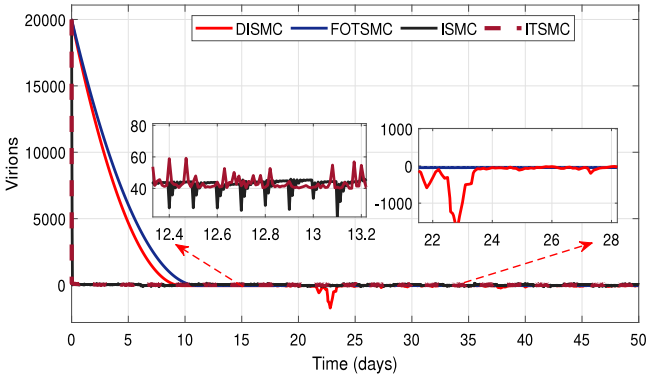

Fig. 12. Behavior of virions in presence of noise.

5.3. Effect of change in parametric value

For the case of FOTSMC, the value of proliferation rate for the infected hepatocytes represented by r_i is increased by 20% and the behavior is shown in Fig. 16. Even with this rise, FOTSMC is capable of achieving the desired reference. Comparing the performance shown in Fig. 6 and Fig. 16, it is clear that the proposed controller is robust against variations in the model parameters.

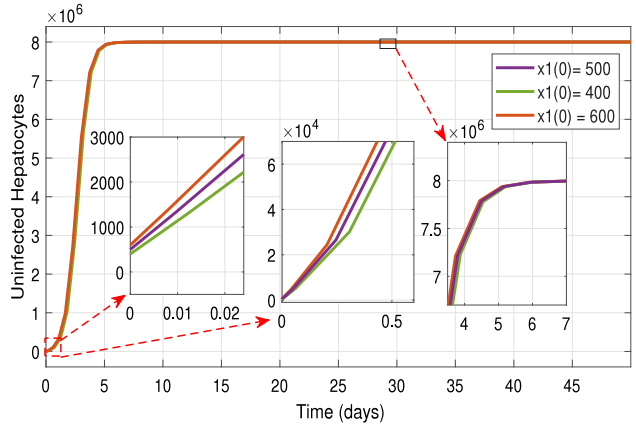

Fig. 13. Different initial conditions uninfected hepatocytes values using FOTSMC.

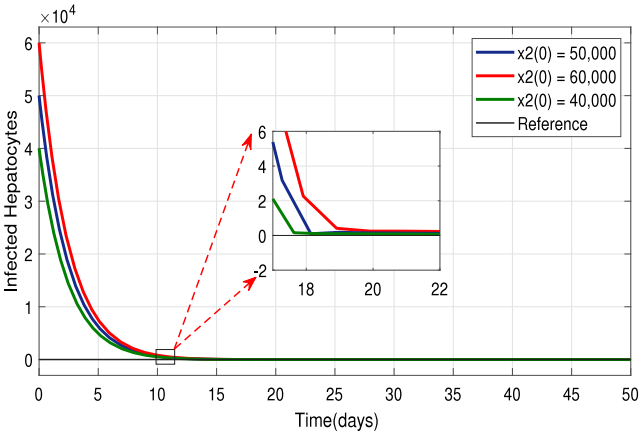

Fig. 14. Different initial conditions infected hepatocytes values using FOTSMC.

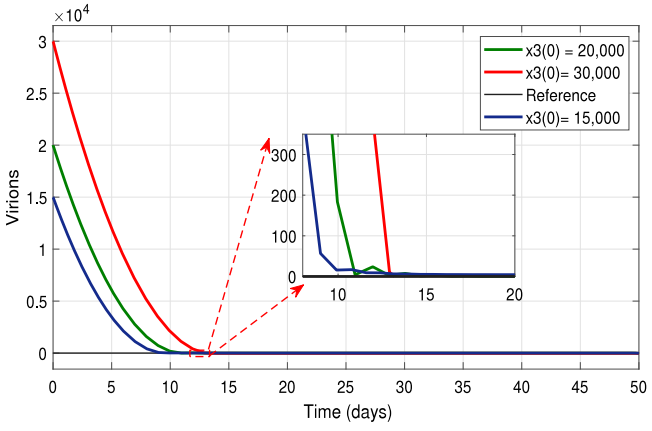

Fig. 15. Different initial conditions virions values using FOTSMC.

6. Conclusion

A combination of ribavirin and peg-IFN-α as control inputs are used for the suppression of virions and infected hepatocytes are based on nonlinear controllers such as FOTSMC, ITSMC, ISMC and DISMC. For blocking and reducing infected hepatocytes and virions to their desired reference values, control input laws have been formulated. Drug efficacy limitations have also been considered in it. From the above-mentioned simulation results, it can be observed that the concentration

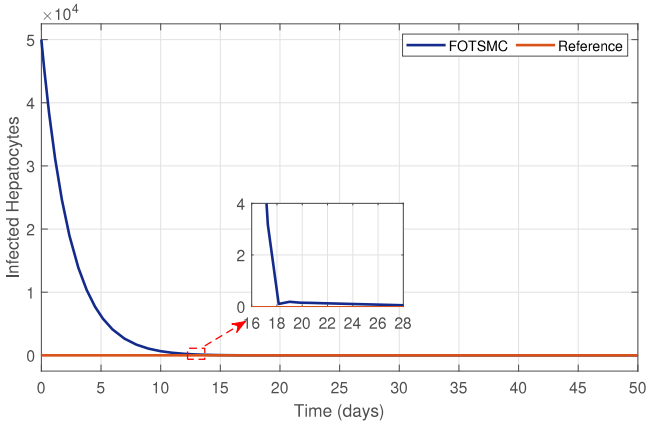

Fig. 16. Infected hepatocytes with variations in model parameter using FOTSMC.

of infected hepatocytes and virions can achieve their respective reference values in almost 10 days. Moreover, it is also depicted here that virions and infected hepatocytes reduce at a faster rate using a combination of ribavirin and antiviral drugs peg-IFN-α. Consequently, uninfected hepatocytes increase automatically and reach to their maximum limit T_{max}. On the basis of undershoots/overshoots, SSE, settling time and transient response, all the nonlinear controllers have been compared with each other. It has been observed that by adding integral action, SSE decreases as can be observed in the case of DISMC. By adding another integral action, SSE has been eliminated completely as shown in the case of FOTSMC. FOTSMC was found better than other proposed controllers and also robust against noise measurement and model parameters. To reduce the un-modeled uncertainties, this work has been further extended by including adaptation.

CRediT authorship contribution statement

Ali Hamza: Conceptualization, Methodology, Software, Data curation, Writing – original draft, Investigation, Validation, Visualization, Project administration. **Muhammad Uneeb:** Conceptualization, Methodology, Software, Data curation. **Iftikhar Ahmad:** Supervision, Validation, Writing – reviewing & editing, Project administration. **Komal Saleem:** Visualization, Writing – reviewing & editing. **Zunaib Ali:** Supervision, Validation, Visualization, Writing – reviewing & editing, Project administration.

Declaration of competing interest

The authors declare that they have no known competing financial interests or personal relationships that could have appeared to influence the work reported in this paper.

Data availability

No data was used for the research described in the article.

References

[1] Q.-L. Choo, G. Kuo, A.J. Weiner, L.R. Overby, D.W. Bradley, M. Houghton, Isolation of a cDNA clone derived from a blood-borne non-A, non-B viral hepatitis genome, Science 244 (4902) (1989) 359–362.
[2] World Health Organization, et al., Global Hepatitis Report 2017, World Health Organization, 2017.
[3] A.U. Neumann, N.P. Lam, H. Dahari, D.R. Gretch, T.E. Wiley, T.J. Layden, A.S. Perelson, Hepatitis C viral dynamics in vivo and the antiviral efficacy of interferon-α therapy, Science 282 (5386) (1998) 103–107.
[4] D. Wodarz, M.A. Nowak, Specific therapy regimes could lead to long-term immunological control of HIV, Proc. Natl. Acad. Sci. 96 (25) (1999) 14464–14469.

[5] M.A. Nowak, S. Bonhoeffer, A.M. Hill, R. Boehme, H.C. Thomas, H. McDade, Viral dynamics in hepatitis B virus infection, Proc. Natl. Acad. Sci. 93 (9) (1996) 4398–4402.
[6] N.M. Dixit, Advances in the mathematical modelling of hepatitis C virus dynamics, J. Indian Inst. Sci. 88 (1) (2012) 37–43.
[7] H. Dahari, A. Lo, R.M. Ribeiro, A.S. Perelson, Modeling hepatitis C virus dynamics: Liver regeneration and critical drug efficacy, J. Theoret. Biol. 247 (2) (2007) 371–381.
[8] Z. Jiang, Design of a nonlinear power system stabilizer using synergetic control theory, Electr. Power Syst. Res. 79 (6) (2009) 855–862.
[9] A. Goyal, Y. Lurie, E.G. Meissner, M. Major, N. Sansone, S.L. Uprichard, S.J. Cotler, H. Dahari, Modeling HCV cure after an ultra-short duration of therapy with direct acting agents, Antiviral Res. 144 (2017) 281–285.
[10] J. Guedj, H. Dahari, L. Rong, N.D. Sansone, R.E. Nettles, S.J. Cotler, T.J. Layden, S.L. Uprichard, A.S. Perelson, Modeling shows that the NS5A inhibitor daclatasvir has two modes of action and yields a shorter estimate of the hepatitis C virus half-life, Proc. Natl. Acad. Sci. 110 (10) (2013) 3991–3996.
[11] J. Guedj, P.S. Pang, J. Denning, M. Rodriguez-Torres, E. Lawitz, W. Symonds, A.S. Perelson, Analysis of hepatitis C viral kinetics during administration of two nucleotide analogues: sofosbuvir (GS-7977) and GS-0938, Antivir Ther 19 (2) (2014) 211–220.
[12] H. Dahari, L. Canini, F. Graw, S.L. Uprichard, E.S. Araújo, G. Penaranda, E. Coquet, L. Chiche, A. Riso, C. Renou, et al., HCV kinetic and modeling analyses indicate similar time to cure among sofosbuvir combination regimens with daclatasvir, simeprevir or ledipasvir, J. Hepatol. 64 (6) (2016) 1232–1239.
[13] Y. Wang, Y. Zhou, F. Brauer, J.M. Heffernan, Viral dynamics model with CTL immune response incorporating antiretroviral therapy, J. Math. Biol. 67 (4) (2013) 901–934.
[14] A. Meskaf, Y. Tabit, K. Allali, Global analysis of a HCV model with CTL, antibody responses and therapy, Appl. Math. Sci. 9 (81) (2015) 3997–4008.
[15] A.M. Elaiw, S.A. Ghaleb, A. Hobiny, Effect of time delay and antibodies on HCV dynamics with cure rate and two routes of infection, J. Appl. Math. Phys. 6 (5) (2018) 1120–1138.
[16] J. Li, K. Men, Y. Yang, D. Li, Dynamical analysis on a chronic hepatitis C virus infection model with immune response, J. Theoret. Biol. 365 (2015) 337–346.
[17] S. Lenhart, J.T. Workman, Optimal Control Applied to Biological Models, Chapman Hall/CRC, 2007.
[18] K. Shao, J. Zheng, H. Wang, X. Wang, R. Lu, Z. Man, Tracking control of a linear motor positioner based on barrier function adaptive sliding mode, IEEE Trans. Ind. Inform. 17 (11) (2021) 7479–7488.
[19] K. Shao, Nested adaptive integral terminal sliding mode control for high-order uncertain nonlinear systems, Internat. J. Robust Nonlinear Control 31 (14) (2021) 6668–6680.
[20] J.M. Ntaganda, M.S.D. Haggar, B. Mampassi, Fuzzy logic strategy for solving an optimal control problem of therapeutic hepatitis C virus dynamics, Open J. Appl. Sci. 5 (09) (2015) 527.
[21] S.P. Chakrabarty, H.R. Joshi, Optimally controlled treatment strategy using interferon and ribavirin for hepatitis C, J. Biol. Systems 17 (01) (2009) 97–110.
[22] S.P. Chakrabarty, Optimal efficacy of ribavirin in the treatment of hepatitis C, Optim. Control Appl. Methods 30 (6) (2009) 594–600.
[23] N.K. Martin, A.B. Pitcher, P. Vickerman, A. Vassall, M. Hickman, Optimal control of hepatitis C antiviral treatment programme delivery for prevention amongst a population of injecting drug users, PLoS One 6 (8) (2011) e22309.
[24] O. Aghajanzadeh, M. Sharifi, S. Tashakori, H. Zohoor, Nonlinear adaptive control method for treatment of uncertain hepatitis B virus infection, Biomed. Signal Process. Control 38 (2017) 174–181.
[25] J. Khodaei-mehr, S. Tangestanizadeh, R. Vatankhah, M. Sharifi, ANFIS-based optimal control of hepatitis C virus epidemic, IFAC-PapersOnLine 51 (15) (2018) 539–544.
[26] J.K. Mehr, S. Tangestanizadeh, M. Sharifi, R. Vatankhah, M. Eghtesad, Hepatitis C virus epidemic control using a nonlinear adaptive strategy, in: Modeling and Control of Drug Delivery Systems, Elsevier, 2021, pp. 1–11.
[27] S. Zeinali, M. Shahrokhi, Adaptive control strategy for treatment of hepatitis C infection, Ind. Eng. Chem. Res. 58 (33) (2019) 15262–15270.
[28] S. Zeinali, M. Shahrokhi, A. Pishro, Observer-based controller for treatment of hepatitis C infection using fractional order model, Math. Methods Appl. Sci.
[29] A. Hamza, I. Ahmad, M. Uneeb, Fuzzy logic and Lyapunov-based non-linear controllers for HCV infection, IET Syst. Biol. 15 (2) (2021) 53–71.
[30] H.K. Khalil, Nonlinear Systems, Upper Saddle River, 2002.
[31] R. Pradhan, B. Subudhi, Double integral sliding mode MPPT control of a photovoltaic system, IEEE Trans. Control Syst. Technol. 24 (1) (2015) 285–292.
[32] M.P. Aghababa, A Lyapunov-based control scheme for robust stabilization of fractional chaotic systems, Nonlinear Dynam. 78 (3) (2014) 2129–2140.
[33] D. Matignon, Stability properties for generalized fractional differential systems, in: ESAIM: Proceedings, Vol. 5, EDP Sciences, 1998, pp. 145–158.
[34] F. Zhang, C. Li, Stability analysis of fractional differential systems with order lying in (1,2), Adv. Difference Equ. 2011 (2011) 1–17.
[35] Z. Gao, X. Liao, Improved oustaloup approximation of fractional-order operators using adaptive chaotic particle swarm optimization, J. Syst. Eng. Electron. 23 (1) (2012) 145–153.
[36] H. Dahari, J.E. Layden-Almer, E. Kallwitz, R.M. Ribeiro, S.J. Cotler, T.J. Layden, A.S. Perelson, A mathematical model of hepatitis C virus dynamics in patients with high baseline viral loads or advanced liver disease, Gastroenterology 136 (4) (2009) 1402–1409.